Ultrasound in Med. & Biol., Vol. 31, No. 7, pp. 919–927, 2005

0301-5629/05/$–see front matter

ELSEVIER

doi:10.1016/j.ultrasmedbio.2005.04.007

● *Original Contribution*

TEMPORAL CALIBRATION OF FREEHAND THREE-DIMENSIONAL ULTRASOUND USING IMAGE ALIGNMENT

MARK J. GOODING,* STEPHEN H. KENNEDY† and J. ALISON NOBLE*
*Wolfson Medical Vision Laboratory, Department of Engineering Science, University of Oxford, Oxford, UK; and
†Nuffield Department of Obstetrics and Gynaecology, The John Radcliffe Hospital, Oxford, UK

(*Received* 6 *December* 2004, *revised* 31 *March* 2005, *in final form* 7 *April* 2005)

Abstract—All freehand 3-D ultrasound systems have some latency between the acquisition of an image and its associated position. Previously, estimation of latency has been made by tracking a phantom in a sequence of images and correlating its motion to that recorded by the position sensor. However, tracking-based temporal calibration uses the assumption that latency is constant between scans. This paper presents a new method for temporal calibration that avoids this assumption. Temporal calibration is performed on the scan data by finding the latency at which the best alignment of the 2-D images within the reconstructed volume occurs. The mean voxel intensity variance is used as a global measure of the quality of alignment within the volume and is minimized with respect to latency for each scan. The new method is compared with previous methods using an ultrasound phantom. Finally, integration of temporal calibration with existing spatial calibration methods is discussed. (E-mail: gooding@robots.ox.ac.uk) **© 2005 World Federation for Ultrasound in Medicine & Biology.**

Key Words: **Freehand, 3-D, Ultrasound, Calibration, Latency, Temporal, Alignment, Compounding.**

INTRODUCTION

Although commercial 3-D ultrasound (US) systems have become more widely available using both mechanically swept probes and, more recently, 2-D phased-array technology, research continues into freehand 3-D US systems. Freehand 3-D US has a number of advantages over the other 3-D probe systems (Fenster and Downey 1996). These advantages include the ability to scan volumes of arbitrary size, accommodating large organs, the flexibility for the operator to select optimal views and to get more data in important areas and the ability to compound images to reduce speckle and artifacts. Freehand 3-D systems use a conventional 2-D US probe in combination with a position sensor, so that the 3-D position of each B-scan can be recorded. A series of B-scans are then reconstructed into a 3-D image in relative positions to allow visualization and processing.

A drawback of research-based freehand US systems is the need for calibration. Spatial calibration, which is required to find the transform of the US image to the position sensor reference frame, is not directly considered in this paper. A review of spatial calibration methods can be found in Mercier et al. (2005). Temporal calibration, which is required to find the association between images and the positions, is addressed in this paper.

Address correspondence to: Dr. M. J. Gooding, Wolfson Medical Vision Laboratory, Department of Engineering Science,University of Oxford, Parks Road, Oxford OX1 3PJ UK. E-mail: gooding@robots.ox.ac.uk

Current temporal calibration methods

Two approaches to temporal calibration are described in the literature. In the first method (Meairs et al. 2000; Prager et al. 1998a), for example, positions and images are continuously recorded while an object is scanned. Initially, the probe is held stationary for a short period. Then a sudden motion is induced in the probe position, causing a noticeable motion of the object within the B-scan. The time at which this motion occurs can be easily detected within both the recorded position and the image sequence, allowing the latency between recordings to be calculated. The latency can only be estimated to an accuracy of $\pm (T + t)/2$ for a single calibration scan, where T is the time between image acquisitions and t is the time between position acquisitions. Because this accuracy is not particularly good, it was suggested by Prager et al. (1998b) that multiple calibrations should be performed and the average latency accepted.

In Burcher (2002) and Treece et al. (2003), this method of calibration is extended to use a constrained but continuous probe motion. Constraining the motion to

a single direction means that spatial calibration need not be performed before temporal calibration. The position of the object within the image is tracked and recorded and the principal direction of motion is found. Similarly, the principal direction of motion of the probe position is found from the uncalibrated positions measurements. The latency is estimated by finding the time offset at which the maximum correlation occurs between the position of the object within the image and the position of the probe, along their principal directions of motion. Interpolation of these positions (both probe and phantom) between recordings can be used to estimate the latency to an accuracy that is significantly better than the resolution of either the image or position acquisitions. Again, averaging of calibration results can be performed to ensure the accuracy of the estimated latency.

Both of these methods make the assumption that the latency being estimated is constant from one scan to the next. The validity of this assumption is required both for averaging calibration results and in the application of the temporal calibration result to subsequent scans.

Latency within different freehand 3-D ultrasound systems

Several variations of freehand 3-D US systems exist, particularly regarding the choice of position sensor. However, the major variation affecting temporal calibration is the way in which the images and positions are acquired by the workstation used for data processing and what facilities exist for matching images to positions. The most common arrangement is that the processing workstation acquires both the images and the positions directly. The images are captured from the US machine video feed using a frame grabber within the workstation and the position is recorded directly by the workstation. Alternatively, the position sensor can be directly coupled to the US machine (Berg et al. 1999) or a personal computer (PC)-based US machine is used (Zhang et al. 2002), allowing the positions to be recorded by the US machine. A third, but largely uninvestigated, method suggested in (Meairs et al. 2000), is that the digital images are recorded by the US machine and then transferred to the processing workstation. The positions are independently recorded by the workstation during the scan. This system has the advantages that the errors in the image data are not introduced during conversion to analogue video and back to digital and that it can be implemented for any digital US machine which has the ability to save digital images in a suitable format to be read by the workstation. Such a system was used for the work in this paper and is described in more detail in the Methods section.

In most freehand systems, the acquisition of images and the acquisition of positions are triggered at approximately the same time. However, unknown latency may exist in both the image-acquisition protocol and the localizer-position acquisition. This can lead to an offset in the time between the first image being acquired and the first position. It is this latency that must be estimated by the temporal calibration process for correct 3-D image reconstruction. However, this latency may vary between scans. For instance, the delay between image acquisition being triggered and the first image being acquired by the US machine is unknown and may not be constant.

Consequently, the assumption of constant system latency made for the temporal calibration methods above may not be valid, leading to an inadequate estimate of latency for accurate reconstruction. In the next section, we present a temporal calibration method that can be applied to each individual scan. This ensures that the correct latency is estimated for every scan. Although this method is illustrated on a freehand US system where the US machine is being used to record images, it is equally applicable to other arrangements of freehand US systems.

MATERIALS AND METHODS

System set-up

The freehand US system used in this work was set up as follows. A 3-D position sensor, a Faro arm (Faro Technologies Inc., Lake Mary, Florida, USA), connected to a PC was used to record the US probe position in 3-D. The probe is rigidly connected to the end of the Faro arm. The PC records positions continuously at 72 Hz after it has been triggered to do so. Images were recorded using the cine function of the US machine (Toshiba Powervision SSA-270, Toshiba Medical Systems, Crawley, West Sussex, UK) to preserve the manufacturer's original image data. Consequently, it was necessary to transfer the images to the PC after the scanning session. A push-through button, as shown in Fig. 1, was used approximately to synchronize the start of image capture with that of position capture. Using this button is similar to knowing that the recording starts at about the same time when a PC is used to record both positions from the position sensor and images from a frame grabber. This button triggers the US machine to start recording images, by directly pressing the US machine cine button. At approximately the same time, an internal keyboard switch is pressed, setting a latched circuit that is monitored by a PC. The PC tests the latched circuit *via* the RS232 port and initiates reading positions when it is set. A screw (see Fig. 1) can be adjusted to ensure that the plunger pushes both the internal keyboard switch and the external cine record button almost simultaneously. Although this button is not strictly necessary to perform calibration, it

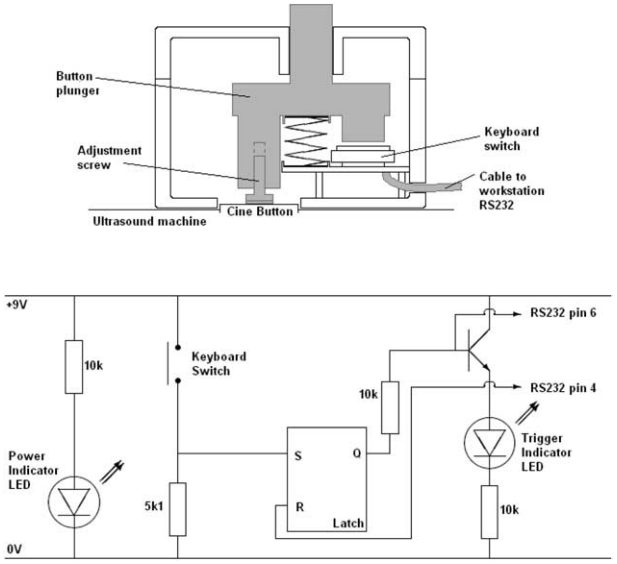

Fig. 1. The push-through switch designed to trigger both cine recording on the US machine and position recording on workstation, which uses the RS232 port to check the latch circuit shown to detect if the switch has been pressed. The circuit is reset by workstation RS232 after recording has finished. The screw shown can be adjusted to ensure that the plunger pushes both internal keyboard switch and external cine record button almost simultaneously.

simplifies the calibration procedure by reducing the temporal search space.

Prelatency estimation processing: Spatial calibration

Spatial calibration was performed using the method described in Atkinson et al. (2001), itself based on the work of Xiao (2001). This calibration uses a cross-wire phantom centered within a table-tennis ball. The center point of the cross-wire could be automatically found, estimating the ball surface position within each image and finding the center of this. Single-image position pairs were captured of the center of the cross-wire while the probe was held still. By holding the probe still for a sufficient time period, the position associated with each image could be estimated, to allow spatial calibration to be performed before accurate temporal calibration. This method of spatial calibration, although quite accurate, is slow. However, spatial calibration is required before the proposed temporal calibration on subsequent data. The integration of the proposed temporal calibration with faster spatial calibration methods is considered in the Discussion section.

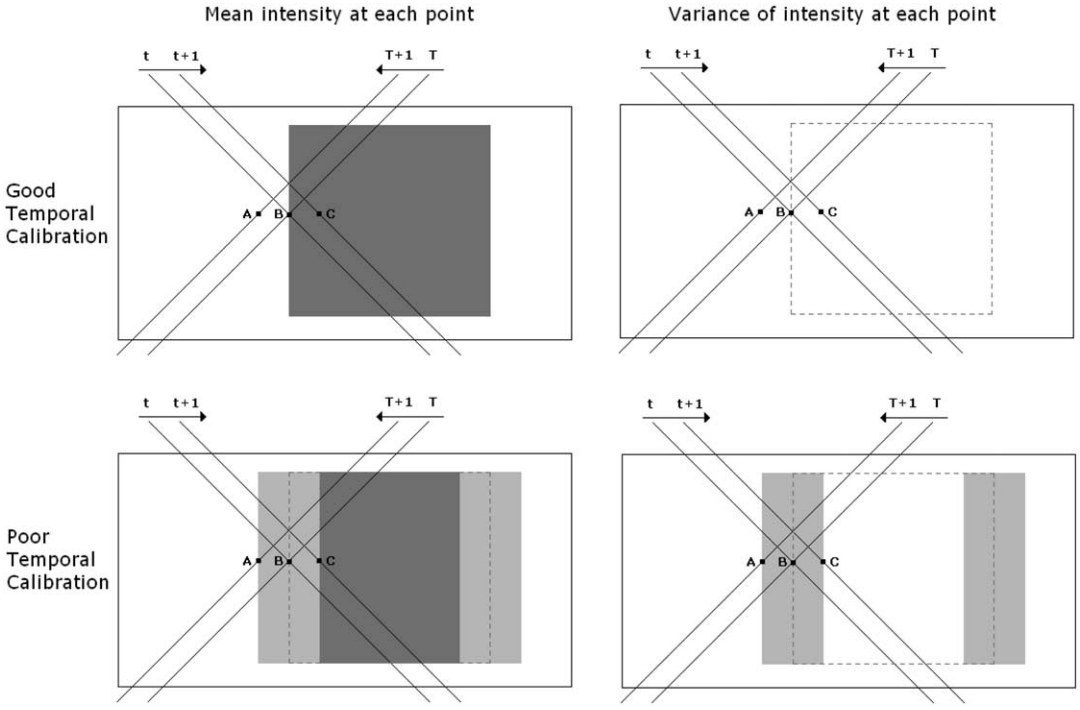

Fig. 2. Illustration shows that latency increases voxel variance for a reconstructed image. For the correct mean intensity image to be generated, as in (top left), image data for point B must be acquired at time t and T. If latency is introduced so that images are acquired at times $t + 1$ and $T + 1$, image data averaged in reconstruction at point B will originate at points A and C. This leads to a variance in the image intensities acquired for this position. Therefore, regions will exist with a higher variance of intensity in each voxel, as shown (bottom right).

An alignment-based temporal calibration method

Temporal calibration using a phantom, as described in Burcher (2002) and Treece et al. (2003), makes the assumption that the latency to be estimated is constant between scans. In the specific acquisition system described above, the US machine was believed to have a variable latency between the cine record button being pushed and the start of image recording. If the latency between the first recorded position and the first image is variable, it is necessary to perform time calibration for each data acquisition. The method presented allows the temporal calibration to be calculated for each new scan, so that the scan-specific latency is estimated.

The ultimate aim of time calibration is to be able to associate images with positions to achieve an accurate 3-D image reconstruction. In a "good" reconstruction, all of the image data used at a point within the 3-D image will be acquired from the same object. Therefore, we expect a similar appearance for image data in each original 2-D B-scan that intersects a 3-D location. This assumption underlies spatial compounding, one motivation for using freehand 3-D (Rohling et al. 1997). To illustrate this, we will consider the simple example shown in cross-section at the top left of Fig. 2. An object consisting of two regions is scanned. One region has a dark homogeneous appearance in the B-scan (the dark grey region), and the other returns a speckled pattern (the white region). The dark diagonal lines represent the B-scans planes for four different times within a continuous scanning period. Times t and T are used for ease of reference and represent different times from the continuous scanning period. The direction of US probe motion at each of these times is shown by the arrows. For an accurate reconstruction, we expect the image at time t to correspond to the plane position shown for time t. Similarly, the image at time T should correspond to plane position shown for time T. Where these image planes intersect, point B, the data in both images should have a similar appearance. Because we expect the image data at any point to have a similar appearance regardless of which B-scan these image data are from, we can perform temporal calibration by assessing the quality of the spatial alignment of the 2-D image structures within 3-D images reconstructed at different latencies.

As with Rohling et al. (1997), we assume that the mean intensity will represent useful image structure and that this measure can be used as a constraint in image compounding. Taking the mean of all the 2-D B-scans pixel intensities intersecting each voxel reduces the SD of intensity in a voxel within a structure, giving regions of approximately homogeneous intensity. This reduces speckle, but preserves objects of interest, provided different viewing angles are used, so that the speckle is decorrelated between images. To assess the quality of 3-D spatial alignment of the 2-D image structures within the reconstructed 3-D image, a reconstruction is performed on a coarse voxel array for each latency being assessed. Both the mean and the variance of B-scan pixel intensities are stored for each voxel within the reconstructed 3-D image. If the image structures are well aligned, that is to say, if the estimated latency is close to the true value, we would expect the intensity variance recorded for each voxel to be low. When the latency is poorly estimated, the variance within each voxel near the image structure boundaries will be higher, because the intensity data will come from more than one intensity structure. Again, we consider the example in Fig. 2. If the latency is estimated correctly, the intensity data used to reconstruct the 3-D image at point B will come from the intensity data for point B in images acquired at times t and T. The voxel intensities, which represent the mean of the 2-D scan intensities at each 3-D location, will, therefore, be correct and the variance associated with each voxel will be zero. Therefore, the voxel intensity image will appear as in the top left of Fig. 2 and the voxel variance image will appear as in the top right of Fig. 2. (Here, white represents zero and grey, nonzero). The dotted line is shown purely to indicate the location of the feature. However, if the latency is estimated incorrectly, so that the images from time $t + 1$ and $T + 1$ are used for plane positions at times t and T, respectively, then the mean of 2-D

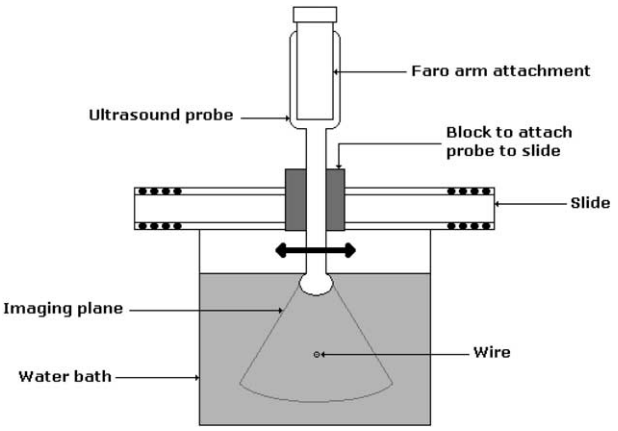

Fig. 3. Temporal calibration performed using a phantom. The probe (with position sensor attached) is constrained to move in a single horizontal direction with the probe oriented so that the imaging plane is parallel to the direction of motion. A fine wire oriented perpendicular to the image plane is scanned in a water bath by moving the probe backward and forward. An iterative search is performed to find the best correlation between the probe position and the position of the needle within the US images.

scan intensities for the voxel at point B will be the mean of intensities acquired from points A and C. Therefore, the complete scan will lead to voxel intensity and variance images, as shown in the bottom left and bottom right of Fig. 2, respectively. Regions exist where the variance of 2-D scan intensities is nonzero. These regions extend around the boundary of the intensity regions in the direction of the probe motion by a distance determined by the error in latency. Taking the mean value of the variance associated with each voxel over the entire volume gives a global measure of the quality of spatial alignment of the 2-D image structures within the 3-D image. This measure is minimized with respect to latency to find the optimum latency associated with the scan.

We performed minimization using an adaptive step-size search, as follows, to find the global minima quickly: The range within which the latency is likely to occur, the maximum time step and the desired temporal accuracy are specified manually. At each time step, a 3-D volume was reconstructed and the mean voxel intensity variance was found for this reconstruction. After this had been done for each time step over the specified range, the range was narrowed to one time step either side of the latency estimate at which the minimum mean voxel variance was found. The search time step was reduced by a manually specified search spacing and the process was iteratively refined until the desired temporal accuracy was reached. For the experiments performed in this paper, an initial range and search spacing of 0 to 2 s in 0.2-s intervals was used. At each iteration, the search spacing was reduced by a factor of five until the minimum search-spacing of 0.01 s was reached. The reconstructions were performed on a voxel grid with 1-mm resolution in each dimension.

Comparative tracking-based calibration method

To compare the proposed temporal calibration method with the state-of the-art, temporal calibration was performed using a phantom in a similar fashion to that of Burcher (2002) and Treece et al. (2003). Following Burcher (2002), the probe (with position sensor attached) was constrained to move in a single horizontal direction with the probe orientated so that the imaging plane was parallel to the direction of motion. A fine wire oriented perpendicular to the image plane was scanned in a water bath by moving the probe backward and forward. The apparatus for this method is shown in Fig. 3. The position of the wire within each image was manually identified to within a few pixels. The accuracy to which the wire location is found is not critical, provided that the error is small compared with the overall change in position within the image series. In our experiments, the position of the wire within the image varied by about 350 pixels. An iterative search was performed to find the best correlation between the probe position and the position of the wire within the US images. We refer to this approach as tracking-based calibration.

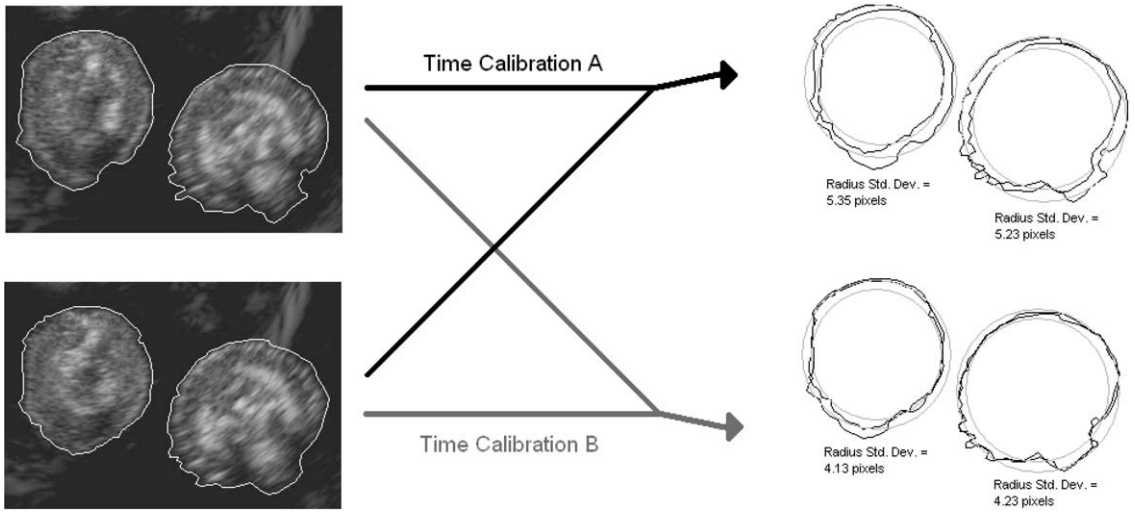

Fig. 4. The aim of time calibration is to find the correct positions for images. If the images are in their correct positions, the boundaries of objects will align better. (above) B-scan images of two grapes; these can be considered as different scans of a single plane through the phantom. (right-hand side) Manually-segmented contours from left-hand images as if they had been positioned onto the appropriate plane of the 3-D image for two different latency estimations. Grey circles show mean radius of the contours ± one SD for each object; SDs are shown beneath. Measuring variance in radius of all boundaries points for reconstructed object gives a measure of boundary alignment. Time calibration B can be seen to perform better than time calibration A because this has lower radius SD for both objects.

Table 1. The tracking-based temporal calibrations for two separate scanning sessions

Session	Temporal calibration 1 (s)	Temporal calibration 2 (s)	Temporal calibration 3 (s)	Temporal calibration 4 (s)	Mean (s)	SD (s)
1	1.37	1.44	1.17	1.19	1.29	0.133
2	1.23	1.16	1.12	1.40	1.22	0.124

Experimental evaluation

For all experiments detailed, 180 2-D B-scan images were acquired at 12.5 Hz and positions were acquired at 72 Hz.

Experiment 1: To examine the variation in latency associated with the freehand system. Four temporal calibrations were performed using the tracking-based method. No adjustment of the equipment was made between scans. A further four tracking-based calibrations were made in a subsequent scanning session. The mean and SD of the latency were computed for each set of four calibrations.

Experiment 2: To assess the accuracy of alignment-based and tracking-based calibration. A phantom was used to test the new calibration method on a real 3-D freehand US scan. Using a phantom has the benefit that the results can be analyzed without concern over other factors that might affect the quality of spatial compounding, such as patient motion (Atkinson et al. 2001; Flaccavento et al. 2004; Rohling et al. 1997). Unlike a simulated scan (*e.g.*, using field II), the phantom scan is subject to the same range of errors (in position measurement, time stamping and US artifacts) as an *in vivo* scan. The phantom consisted of two peeled seedless grapes suspended in gelatin. The two regions within scans of this phantom are similar in US appearance to the tissue types found in a breast cyst scan or ovarian follicle scan, one anechoic region and one uniformly textured region.

Reconstruction of the data were performed using the calibration from the new alignment-based temporal calibration method proposed. This reconstruction was compared with a reconstruction using the mean latency found from two tracking-based temporal calibrations performed at the time of scanning the grape phantom. Comparison was performed, qualitatively, by examining a cross-section through the compound 3-D image to assess relative sharpness of the object boundary for different latency estimates.

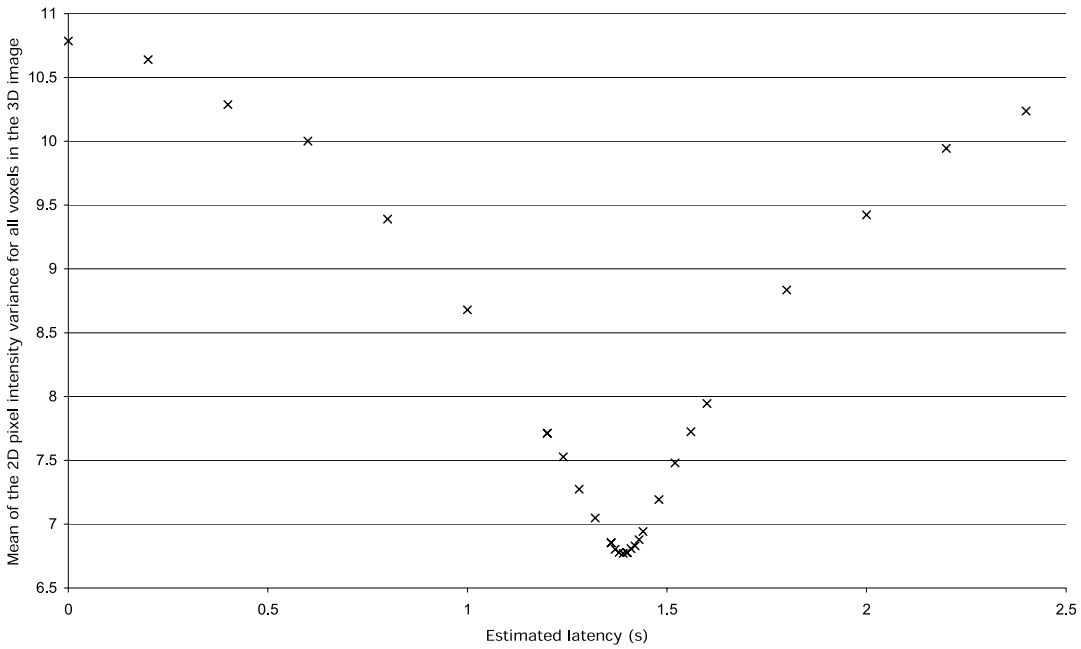

Fig. 5. Measurement of spatial alignment of image structures by considering the mean of the pixel intensity variance for each voxel in a coarse 3-D reconstruction. The mean voxel variance is plotted against latency, with minima found at a latency of 1.39 s. At the latency estimated using tracking-based calibration (1.18 s), the mean voxel variance is noticeably higher than the minimum.

Quantitative assessment was performed by measuring the spatial alignment of manually-delineated object boundaries within the reconstructed volume, illustrated in Fig. 4, because our goal was to achieve better spatial alignment of image structures by improving the temporal calibration. Manual delineation was done on each 2-D frame of the US scan and reconstruction of these 2-D boundaries into a volume was performed at different latencies. Although the manual segmentation is subjective, it does not introduce bias into the result, because the person segmenting is unaware of the spatial position that each image will occupy within the reconstructed volume at each latency. The degree to which the boundaries were aligned in the volume was assessed in the following automatic way. For each object, the center was found as the point that minimized the variation in radius from this point. Minimization was performed using a gradient descent algorithm. The mean of the variance of the radius for all objects was taken as a measure of boundary alignment within the volume. Some variation is introduced by intraobserver error in the segmentation and by natural variation in the radius of the grape. This natural variance exists for all latencies and does not effect the minimization. Consider Fig. 4, where there exists some difference between the two outlines of each grape and neither grape is spherical: this results in some variance in radius for the well-aligned images. However, the misalignment as a result of incorrect latency estimation increases the variance in radius. Radii were measured in terms of the real distance to the object center (*i.e.*, position of each boundary point was calculated in 'real' space using the plane position and spatial calibration parameters without requiring use of voxel array and distances were measured within this "real" space) (Zhang et al. 2002). Although this method could potentially be used for temporal calibration itself, the need manually to delineate boundaries makes this impractical.

RESULTS

Experiment 1

Table 1 shows the four estimated latencies found using the tracking-based calibration method for both scanning sessions. For both sessions, the latency had a SD of about 0.13 s. This variability means that the temporal calibration could be wrong by up to three position recordings in either direction for *in vivo* scans using the mean temporal calibration.

Experiment 2

The latency found using alignment-based calibration was 1.39 s for the grape phantom scan. Figure 5 shows the mean intensity variance for the voxels in the coarse 3-D reconstruction plotted against the estimated latency. The tracking-based temporal calibrations estimated the latency to be 1.18 s (readings of 1.25 s and 1.11 s). Cross-sections through the reconstructed 3-D image of the grape phantom are shown in Fig. 6. The intensity of each voxel within the reconstruction was set to be the mean of the 2-D B-scan pixel intensities intersecting that voxel. The first row shows the two original B-scan images. The subsequent rows show cross-sections through the 3-D image at equivalent positions to the original images after the various time calibrations, with no software-based calibration (assuming the trigger switch is 100% accurate), using tracking-based calibration and using alignment-based calibration. Although both temporal calibration methods show the ability to remove speckle in the compound image, the alignment-based calibration preserves detail better than does the tracking-based calibration. Particular attention is drawn

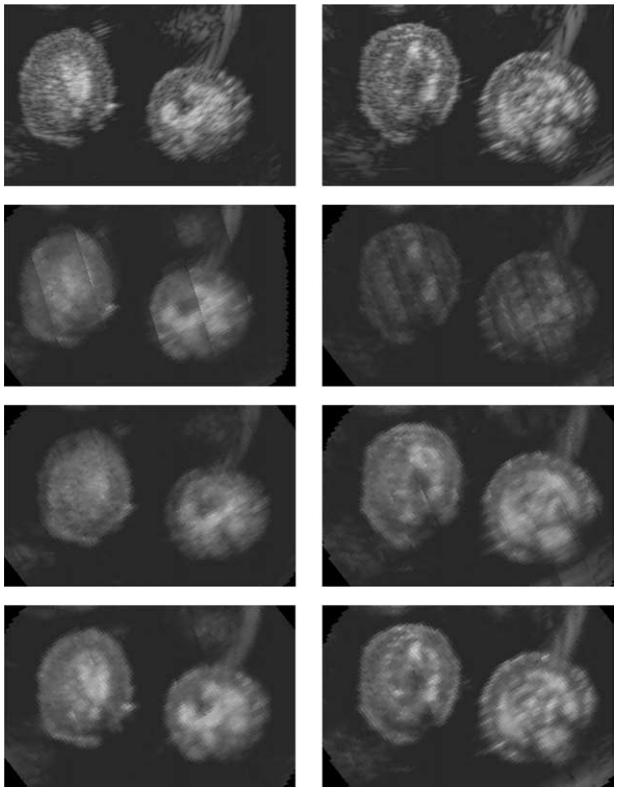

Fig. 6. Cross-sections through the reconstructed 3-D image compared with the original image. (first row) Original images. (second row) Image cross-section through 3-D image reconstructed without temporal calibration. (third row) Image cross-section through 3-D image reconstructed using result of tracking-based temporal calibration (t = 1.18 s). (fourth row) Image cross-section through 3-D image reconstructed using alignment-based temporal calibration (t = 1.39 s). Particular attention is drawn to top right boundary and center detail of each grape. Reconstruction using alignment-based temporal calibration removes speckle by compounding and preserving image detail better than reconstruction using tracking-based calibration.

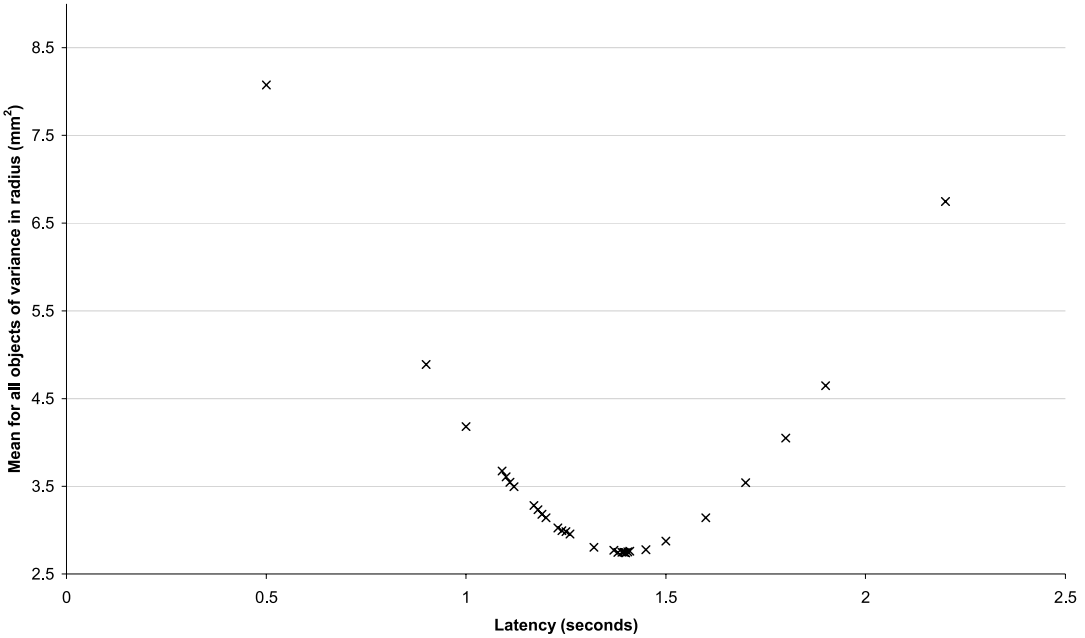

Fig. 7. Mean variance in radius for objects within the 3-D image plotted against the latency used in reconstruction. The best alignment of boundaries is found at a latency of 1.4 s. This is 0.01 s from the latency estimated using alignment-based temporal calibration. At the latency estimated using tracking-based calibration (1.18 s), mean variance in radius is noticeably higher than the minimum.

to the upper boundary of the grapes, where the stronger surface reflection is weakened by misalignment in the reconstruction using tracking-based calibration. This stronger reflection can be seen in the compound image after alignment-based calibration. Likewise, detail in the center of the grapes can be seen to be better preserved in the reconstruction after alignment-based calibration.

Figure 7 shows a plot of the mean variance in radius of the two grapes within the 3-D image against the latency used in the reconstruction. The minima for this variance and, hence, the time at which the best alignment of the manually-delineated boundaries occurs, is found at a latency of 1.40 s. This minimum shows about 2.5 mm^2 variance in radius, because the grapes are nonspherical and, therefore, the radius of each grape varies over its surface. The variance in radius was found to be much higher at the times found by tracking-based calibration than at the time found by alignment-based temporal calibration. The latency estimated by tracking-based calibration was the equivalent of about three position measurements wrong for each image (0.21 s), whereas the alignment-based calibration performs well, with an error equivalent to less than one position recording wrong (0.01 s).

DISCUSSION

The freehand acquisition system used in this paper was designed to be able to use the manufacturer's digital images to improve image quality. However, this set-up resulted in significant variability in latency within the system. We have shown that accurate estimation of this latency and, consequently, accurate 3-D image reconstruction, cannot be achieved if tracking-based temporal calibration is used because this does not estimate the latency for each acquisition. A method was presented to overcome this problem by performing temporal calibration on each scan. Calibration was achieved by measuring the quality of spatial alignment of the individual 2-D images within the 3-D image. Spatial alignment was measured by considering the mean intensity variance of voxels on a coarse reconstruction. This measurement assumes that the interesting structure within each image is represented by a homogeneous grey-level intensity. This assumption will not hold in all scans, such as in the scanning of tumors identified by texture, but is appropriate in many cases.

The new method was qualitatively shown to improve the preservation of image detail, compared with tracking-based calibration. Quantitatively, it was shown that the latency estimated is very close to the time at which the boundaries of the objects are best aligned. Unlike tracking-based temporal calibration, the method described requires prior spatial calibration. For spatial calibration based on the acquisition of multiple individual images, such as the crosswire phantom described above, calibration can be performed using the method

described previously in the paper before temporal calibration. The probe is held still for a significant period of time while each image is acquired. The positions can then be averaged over the time for which the probe was stationary in order to obtain a good estimate of the probe position for each image acquisition. However, faster spatial calibration methods require continuous scanning and, therefore, temporal calibration must be done first (*e.g.*, Prager et al. 1998b). The tracking-based temporal calibration can easily be performed in the same scan as the spatial calibration by ensuring that the scan starts with a single linear direction. The latency estimated within the scan will be appropriate for use with the spatial calibration. After spatial calibration has been performed, the subsequent freehand scans can use the proposed method to perform accurate temporal calibration.

SUMMARY

In this paper, we present a method to address the problem of variable latency within freehand US systems. The proposed solution involves measuring the quality of spatial alignment of the individual 2-D images within a 3-D voxel volume. The mean voxel intensity variance in the volume was used as a global measure of the quality of spatial alignment. The method presented was shown to perform better, both qualitatively and quantitatively, than the mean of estimates from tracking-based temporal calibration.

Acknowledgements—M. J. Gooding was funded by the EPSRC as part of the MIAS-IRC (GR/N14248). The authors thank Toshiba Medical systems for the generous provision of a Powervision US machine for this research.

REFERENCES

Atkinson D, Burcher M, Declerck J, Noble JA. Respiratory motion compensation for 3-D freehand echocardiography. Ultrasound Med Biol 2001;27(12):1615–1620.

Berg S, Torp H, Martens D, et al. Dynamic three-dimensional freehand echocardiography using raw digital ultrasound data. Ultrasound Med Biol 1999;25(5):745–753.

Burcher M. A force-based method for correcting deformation in ultrasound images of the breast. Ph.D. thesis. Dept. Engineering Science, University of Oxford, 2002.

Fenster A, Downey DB. 3-D ultrasound imaging: A review. IEEE Eng Med Biol 1996;15(6):41–51.

Flaccavento G, Lawrence P, Rohling RN. Patient and probe tracking during freehand ultrasound. Lecture Notes in Computer Science. Proc MICCAI 2004;3217:585–593.

Meairs S, Beyer J, Hennerici M. Reconstruction and visualization of irregularly sampled three- and four-dimensional ultrasound data for cerebrovascular applications. Ultrasound Med Biol 2000;26(2):263–272.

Mercier L, Langø T, Lindseth F, Collins LD. A review of calibration techniques for freehand 3-D ultrasound systems. Ultrasound Med Biol 2005;31(2):143–165.

Prager RW, Gee AH, Berman LH. Stradx: Real-time acquisition and visualization of freehand three-dimensional ultrasound. Med Image Anal 1998a;3(2):129–140.

Prager RW, Rohling RN, Gee AH, Berman LH. Rapid calibration for 3-D freehand ultrasound. Ultrasound Med Biol 1998b;24(6):855–869.

Rohling RN, Gee AH, Berman LH. Three-dimensional spatial compounding of ultrasound images. Med Image Anal 1997;1(3):177–193.

Treece GM, Gee AH, Prager RW, Cash CJC, Berman LH. High-definition freehand 3-D ultrasound. Ultrasound Med Biol 2003; 29(4):529–546.

Xiao G. 3-D free-hand ultrasound imaging and image analysis of the breast. Ph.D. thesis. Dept. Engineering Science, University of Oxford, 2001.

Zhang Y, Rohling R, Pai DK. Direct surface extraction from 3D freehand ultrasound images. In: Proceedings of IEEE visualization, Boston, MA, October 2002. Washington, DC: IEEE, 2002.